Irradiation Wavelength Selective Surface Modification of a Triazeno Polymer

T. Lippert,*,† T. Nakamura, H. Niino, and A. Yabe

National Institute of Materials and Chemical Research, Laser Induced Reaction Lab, Higashi 1-1, Tsukuba, Ibaraki 305, Japan

Received November 20, 1995; Revised Manuscript Received May 21, 1996[⊗]

ABSTRACT: Standard spectroscopic and surface analysis techniques were used to study a triazeno polymer after laser treatment. Two different excimer lasers, KrF at 248 nm and XeCl at 308 nm, were applied as irradiation sources. For both excimer lasers fluences below and above the threshold of ablation were used. In the case of fluences below the threshold of ablation the irradiation led to a decrease of the absorption of the triazeno chromophore. From XPS spectrum and contact angle measurements a surface oxidation of the polymer is identified. After irradiation with fluences above the threshold of ablation for both irradiation wavelengths a different behavior is observed. Irradiation with the XeCl laser led to a less pronounced surface roughening as compared to KrF laser treatment. With the XPS and contact angle measurements, only slight changes could be detected. A totally different behavior was found for irradiation with the KrF excimer laser. The surface of the polymer turned black after the irradiation, and the oxygen and nitrogen content is drastically reduced, as determined from the XPS spectrum. The SEM pictures revealed the appearance of microstructures of about 5 μm size with some "treelike" structures at the top of the "naps". Contact angle measurements show also the existence of a nonpolar surface. Spectroscopic techniques showed that there exists a clear difference between the irradiation of the triazeno polymer at the two wavelengths under ablation conditions. Excitation of the triazeno chromophore at 308 nm leads to clear ablation, whereas the irradiation with 248 nm introduces microstructures and a carbonized surface.

Introduction

The use of lasers in polymer science has become a vast field of interest.[1] Lasers are used as analytical tools and for many applications such as material processing and information storage. Material processing applications have become available with the advent of high-energy pulsed lasers. Excimer lasers are particularly interesting for structuring of polymers in a one-step dry etching process.[2] This application is closely related to the ablation of polymers, a process first reported in 1982.[3] Since the first reports, numerous studies have been published, but there is still no generally accepted mechanism of polymer ablation. The different suggestions are thermal, photothermal, and photochemical mechanisms and/or a mixture of these.[4−6]

In most studies of polymer ablation, standard polymers were used. A novel and different approach was the development of photopolymers designed for ablation[7] at a specific laser irradiation wavelength. This concept combines two different ideas: application of laser ablation for high-resolution lithography and development of "dry-etching laser photoresists". The triazeno polymers were developed as mid- to deep-UV photoresists for laser irradiation, which has two advantages over the lamp techniques of today: lasers result, due to the shorter wavelengths, in higher resolution, and lasers have the potential (high energy) to be used for a dry etching process (ablation). In addition lasers are the easier (cheaper) high-resolution dry etching technique as compared to other candidates like X-ray, electron, or ion beam.

The triazeno polymers consist of a photolabile N═N−N (triazeno) group in the main chain of the polymer and have an absorption maximum around 300 nm. The tailoring of the absorption properties and photodecomposition behavior for a specific laser wavelength was the second idea behind the development of the triazeno polymers. In this case the polymer was designed for the use of a XeCl excimer laser with an emission wavelength of 308 nm. From the introduction of a photolabile group in the polymer main chain, with preferred positions of the bond breaking, information about the importance of the photochemical mechanism was expected. Gaseous photodecomposition products, such as nitrogen, can act as driving and carrier gases of ablation.[8] Therefore, other products are transported away from the polymer surface to overcome the problem of redeposited material. This so-called debris can contaminate the surface or irradiation mask, reducing the etching resolution and necessitating additional cleaning steps.[9]

In previous communications of this project the synthesis[10] and decomposition behavior[11] of some triazeno polymers were studied. The polymers have a typical molecular weight of about 70 000, are stable up to 550 K or more, and can be stripped off with aqueous acidic solutions.[12] The properties of the polymers, such as absorption maximum, quantum yield of decomposition, and decomposition temperature, can be controlled by varying structural parameters, mainly the bridging group between the aromatic groups.[12] The tailoring of the absorption properties allows the use of specific shorter wavelengths (e.g. 248 or 193 nm) which have the potential for a higher resolution. It was shown that the polymers can be structured with high resolution which is close to the diffraction limited resolution of 0.4 μm at 308 nm (for our set up).[13] The other important feature was the total lack of surface contamination,[13] which demonstrates that the triazeno polymers can be used as "true" dry etching resists with no additional cleaning steps. Also the etch rates with 308 nm irradiation were higher than those for 248 nm irradiation,

* To whom correspondence should be addressed.

† Present address: Los Alamos National Laboratory, Division of Chemical Science and Technology, CST 6, MS-J 585, Los Alamos, NM 87545. Fax: (505)-665-4817. E-mail: lippert@lanl.gov.

⊗ Abstract published in *Advance ACS Abstracts,* August 15, 1996.

S0024-9297(95)01719-0 CCC: $12.00

Chart 1. Structural Unit of the Triazeno Polymer

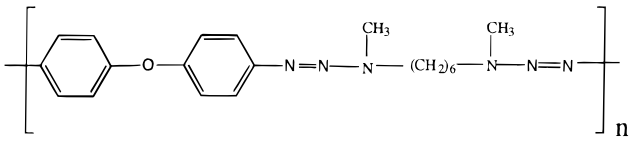

in spite of the higher absorption coefficient at 308 nm and therefore the lower laser penetration depth.[7] This specific behavior is suggested to be a result of dynamic optical properties and a larger contribution of the thermal mechanism with 248 nm irradiation,[14] but also shows that our concept of tailoring the photolabile polymers for a specific irradiation wavelength is working.

In this study, surface and standard analytical techniques were used to study one selected polymer (shown in Chart 1) after laser irradiation at 248 and 308 nm to get more information about the acting mechanism. In addition the potential of UV laser irradiation for selective polymer surface modification was probed.

Experimental Section

Materials. The polymer was synthesized according to a procedure described elsewhere.[10] Thin films of various thicknesses were prepared using the solvent casting technique with spectroscopic grade solvent (chloroform, Aldrich). As substrate, either glass or quartz wafers were used. The homogeneity of the films was tested by recording the UV spectrum at different positions of the wafer with a spatial resolution of 5 mm.

Instrumentation. Irradiation of the polymer films was carried out using a Lambda Physik EMG 102 MSC excimer laser at 308 nm and a Lambda Physik EMG 201 MSC excimer laser at 248 nm. The energy was measured with a Gen-Tec joule meter, model ED 500. The UV spectra were recorded on a Shimadzu UV 2100 spectrometer.

Fourier transform (FT) Raman spectra were recorded on a JEOL IR 7000 spectrometer, using a silver plate under the samples to enhance the spectrum intensity. Most spectra were recorded in the focused mode of the spectrometer, using 100 mW laser energy. To avoid thermal damage of the treated polymer surface the defocused mode with 10 mW energy was used also.

The scanning electron microscopy (SEM) pictures were taken on a TOPCON DS 720 instrument. X-ray photoelectron spectroscopy (XPS) and secondary ion mass spectrometry (SIMS) experiments were done with a Perkin-Elmer Phi 5600 instrument.

Results

UV Spectroscopy. Thin films of the polymer (100−350 nm) were cast on quartz wafers. It was not possible to use thicker polymer films due to the high absorption coefficient of the polymer (166 000 cm^{-1} at 308 nm and 66 000 cm^{-1} at 248 nm).

For fluences above the threshold of ablation (32 mJ cm^{-2} at 248 nm and 22 mJ cm^{-2} at 308 nm)[14] the film was ablated nearly completely after a few pulses and no absorption was detected in the range 230−500 nm, whereas below 230 nm some absorption remained. An optical inspection of thicker films cast on quartz, which could not be used in the UV spectrometer, revealed a pronounced difference between irradiation with 248 and 308 nm.

After irradiation with 308 nm only a slight loss of transparency could be seen, whereas after irradiation at 248 nm the films turned black. This behavior was found at various repetition rates (1−40 Hz) and for different substrates (glass and quartz). This shows that the appearance of the polymer film after irradiation is not due solely to thermal effects of the substrate or cumulative heating effects of the laser pulses. The blackening of the surface[15] after irradiation with 248 nm was never found for 308 nm irradiation, even for high repetition rates and glass as substrate, showing that for each wavelength a different mechanism is acting.

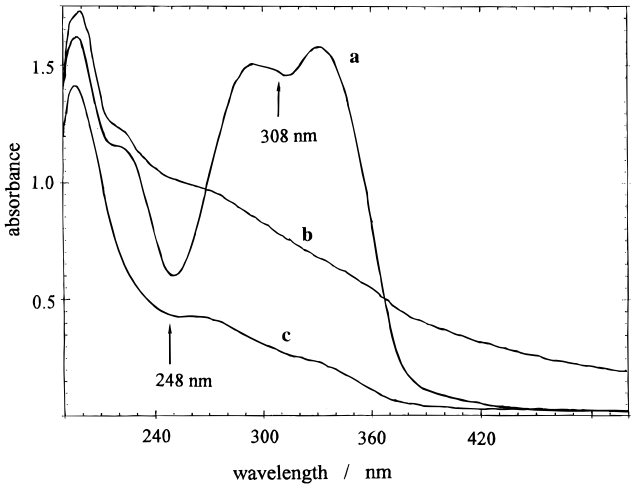

Figure 1. UV spectrum of the untreated polymer film on a quartz wafer (a), thickness about 200 nm, (b) after irradiation with 10 mJ cm^{-2} (2000 pulses) at 308 nm, and (c) after irradiation with 9 mJ cm^{-2} (500 pulses) at 248 nm.

For the fluences below the threshold of ablation a different behavior after irradiation with the two wavelengths was found also. With 248 nm irradiation the absorption decreased continuously, as shown for 500 pulses in Figure 1c. In the case of the 308 nm irradiation first the absorption decreased, to a curve similar to that shown for 248 nm irradiation in Figure 1c. After more than 250 pulses an overall increase of the absorption is detected (shown in Figure 1b for 2000 pulses). An optical inspection of the sample revealed a loss of transparency and an opaque appearance. The broad appearance of the absorptivity suggests that the increase of the absorption is due to a scattering process. To decide whether this is due to an increase of surface roughness, the films were examined with scanning electron microscopy (SEM).

SEM. SEM pictures were taken after irradiation at both wavelengths with fluences below and above the threshold of ablation after various numbers of pulses.

After irradiation at both wavelengths with fluences below the threshold of ablation *no* changes of the surface morphology could be detected.

A totally different behavior was observed for the higher energies. After 308 nm irradiation with 30 mJ cm^{-2} roughening of the surface was detected. The microstructures reached a maximum intensity after about 10 pulses (Figure 2a) and got less pronounced with successive pulses, as shown for 60 pulses in Figure 2b. The microstructures which appear as holes in the pictures have a diameter of about 1 μm.

In the case of 248 nm irradiation the surface appeared different. A well-pronounced "nap" structure is detected (Figure 3a) with growing nap sizes. After 250 pulses (shown in Figure 3b) the naps reach a size of about 5 μm. On the top of the naps additional material is detected, which grows in some cases to "tree like" structures (shown in Figure 3c). It can also be seen that this material did not cover the surface completely.

Contact angle. To study whether chemical modifications take place, in addition to the physical changes

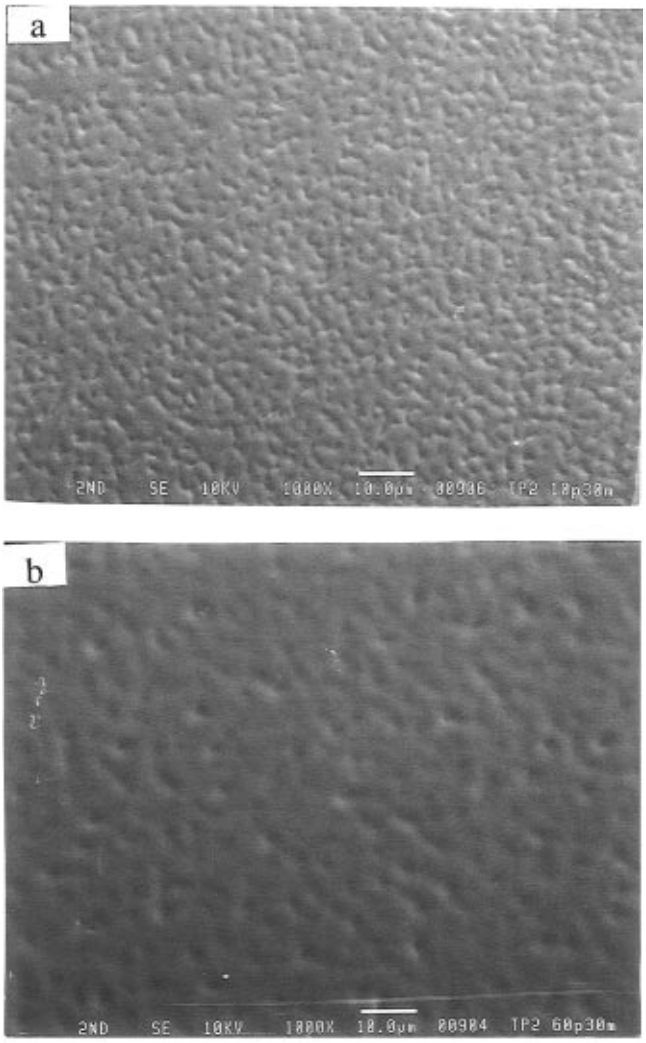

Figure 2. Scanning electron micrographs of surface changes: (a) after 10 pulses with 30 mJ cm^{-2} at 308 nm; (b) after 60 pulses with 30 mJ cm^{-2} at 308 nm.

of the surface, contact angle measurements were used. For both irradiation wavelengths, again, fluences below and above the threshold of ablation were used, and the contact angle of water was measured directly after the irradiation.

For the fluences below the threshold of ablation a similar behavior for both irradiation wavelengths was observed. The contact angle decreased from 57.5 to about 20° (Figure 4). The SEM pictures have shown that no surface roughening took place which could cause a decrease of contact angle.[16] Therefore the change of the contact angle is due to chemical alteration of the surface.

In the case of the higher irradiation fluence different behavior is observed (Figure 5). For 308 nm irradiation the contact angle decreased only slightly. This is in agreement with the SEM pictures (Figure 2) which show a slight roughening of the surface. With 248 nm irradiation more complex behavior is observed. First the contact angle decreased, due to the observed growth of the microstructures. After more than 5 pulses the trend changes and the contact angle increased drastically, although the SEM pictures show the development of more pronounced microstructures. Therefore, a large change in the surface polarity must be the reason for this behavior. For more than 60 pulses the surface appears black and the contact angle becomes time

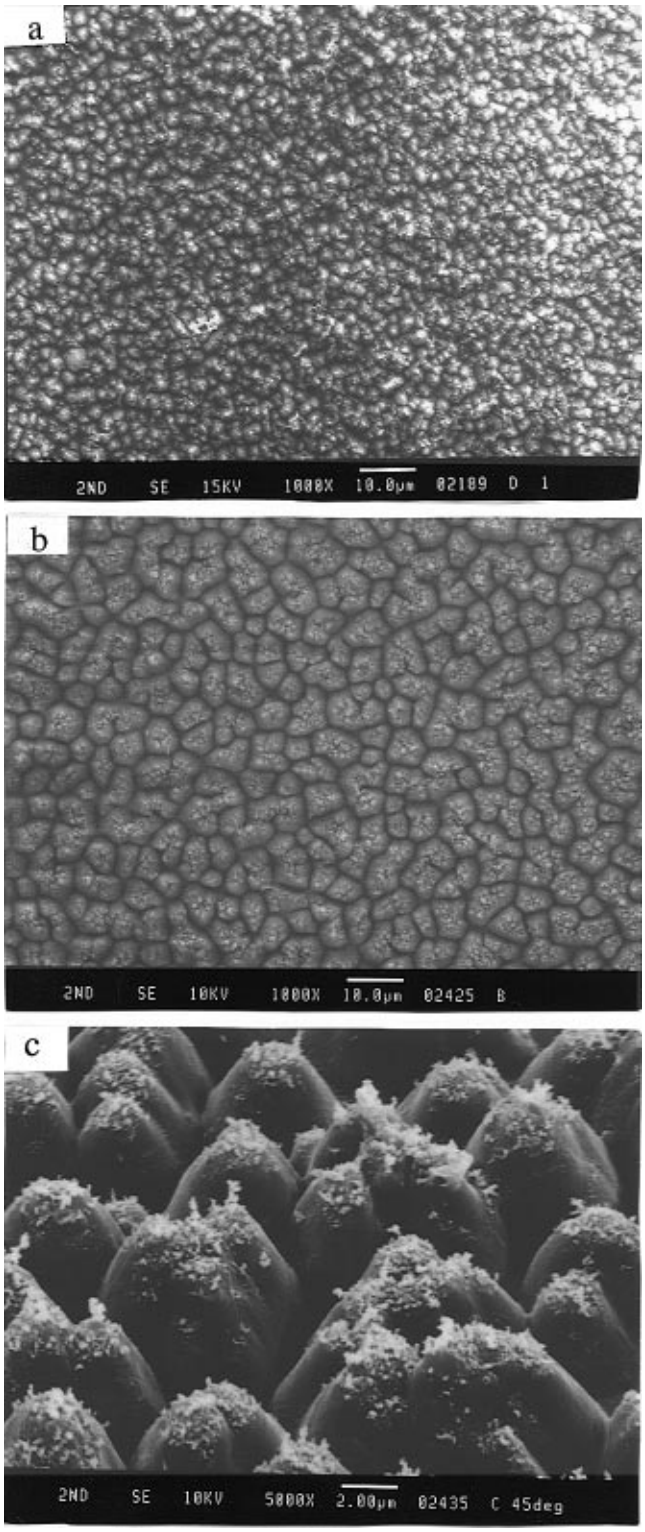

Figure 3. Scanning electron micrographs of surface changes: (a) after 10 pulses with 36 mJ cm^{-2} at 248 nm; (b) after 250 pulses with 36 mJ cm^{-2} at 248 nm; (c) enlarged view of (b) at 45°.

dependent. If the contact angle is measured immediately after the irradiation, values of about 80° result, but also fast darkening of the water droplet and a decreasing angle are observed. If the contact angle is measured after 24 h or more, the values are constant at about 140° and the water droplet does not turn black.

FT-Raman Spectroscopy. In order to get information about the observed chemical changes of the surface FT-Raman spectroscopy was used to examine the surface after laser irradiation. Due to the high penetration

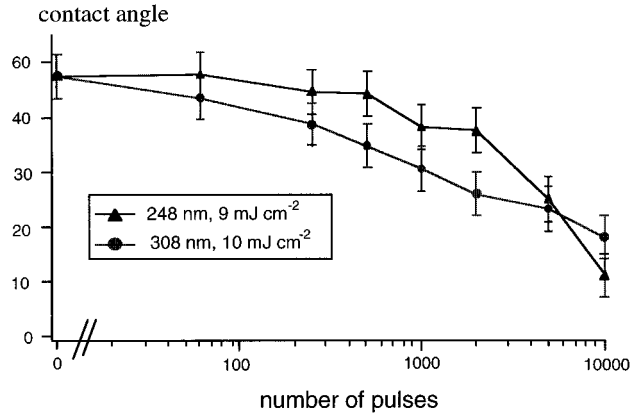

Figure 4. Changes of the water contact angle after irradiation with fluences below the threshold energy of ablation. Irradiation with various pulse numbers at 248 and 308 nm.

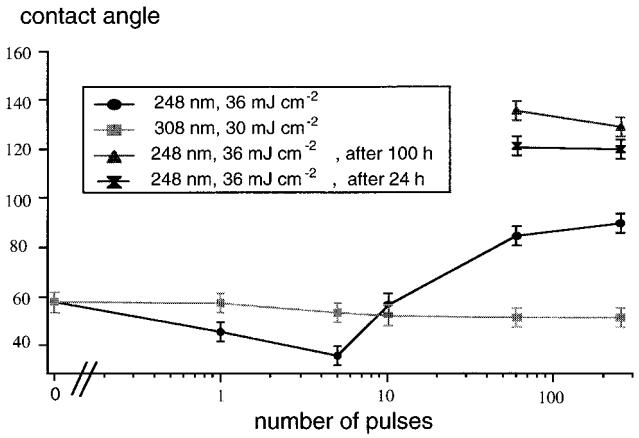

Figure 5. Changes of the water contact angle after irradiation with fluences above the threshold energy of ablation. Irradiation with various pulse numbers at 248 and 308 nm.

depth of the Nd:YAG laser beam of the spectrometer we were well aware that possible information would mainly consist of bulk properties. But, nevertheless, the spectra are valuable because there is also a large possibility of decomposition, especially of the triazene chromophore in the bulk. Raman spectroscopy was used, as compared to IR spectroscopy, because of the less complex band structure of the polymer and the larger Raman cross section of the N=N—N chromophore. Measurements with normal Raman spectroscopy were not possible, due to a high fluorescence background with the use of visible excitation light.

In Figure 6 the Raman spectra of the polymer are shown: (a) before irradiation, (b) after 10 000 pulses at 308 nm with 10 mJ cm^{-2}, (c) after 1000 pulses at 248 nm with 9 mJ cm^{-2} (both are below the threshold of ablation), (d) with 250 pulses at 308 nm with 30 mJ cm^{-2}, and (e) with 60 pulses at 248 nm with 36 mJ cm^{-2}. Spectra a—d are all measured under the same conditions, using films of about 3 μm thickness on glass. Additionally, a silver plate was used under the glass to increase the intensity. The laser for this measurement was used in the "spot" (100 mW) mode of the instrument, giving higher intensities. For each of these spectra 56 scans were accumulated. In the case of spectrum e it was necessary to change to the "defocused mode" (10 mW) of the spectrometer, because in the focused mode the "black" surface disappeared after a few scans, due to the high thermal load. Therefore, the defocused mode was used and 1000 scans were accumulated. The peaks marked with an asterisk are due

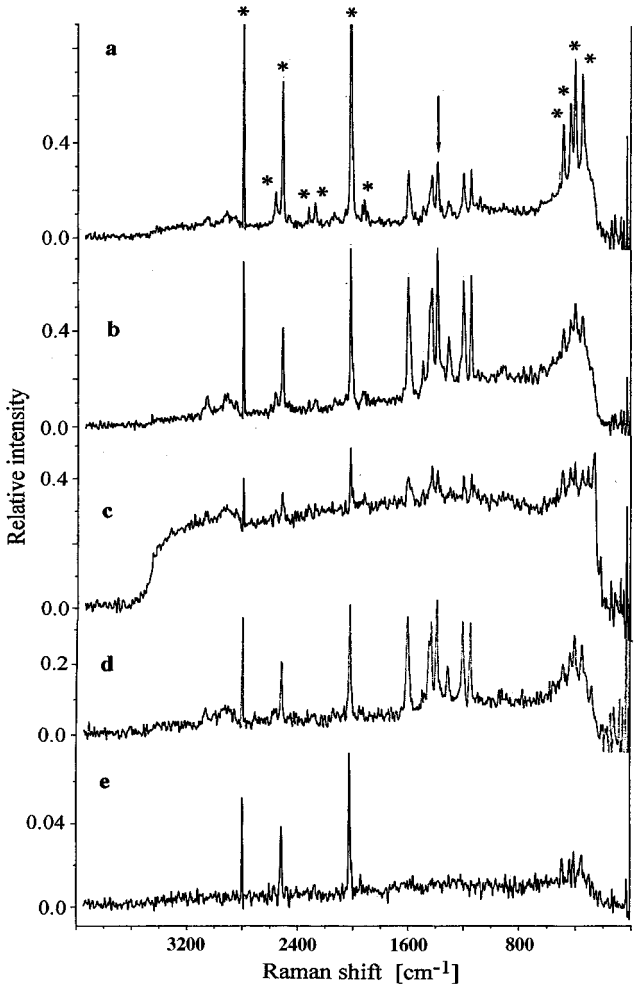

Figure 6. FT-Raman spectra (a) of the untreated polymer, (b) after 10 000 pulses with 10 mJ cm^{-2} at 308 nm, (c) after 1000 pulses with 9 mJ cm^{-2} at 248 nm, (d) after 250 pulses with 30 mJ cm^{-2} at 308 nm, and (e) after 60 pulses with 36 mJ cm^{-2} at 248 nm. The asterisks indicate the background and the arrow marks the N=N—N band.

to the laser and the substrate (background). The peak with the highest intensity of the polymer at 1392 cm^{-1} was assigned to the triazeno chromophore, according to comparison with data of monomeric triazeno compounds[17] and the expected high Raman cross section of the N=N bond.

After irradiation with 10 000 pulses with 10 mJ cm^{-2} at 308 nm (b) an increase of the bands corresponding to the polymer is detected, whereas the "background" decreases slightly. No new bands could be detected, and the peak ratios remain constant.

Irradiation with 9 mJ cm^{-2} at 248 nm (1000 pulses) revealed different behavior, showing that the slight loss of optical transparency is due to a different reason. The increase of the baseline (c) is a typical feature for a thermal load of the sample caused by some absorption of the near infrared (NIR) excitation laser.[18] It also appears that the intensity of the band assigned to the triazeno chromophore decreased more than the other bands.

After irradiation with 30 mJ cm^{-2} at 308 nm behavior similar to that for the low energy irradiation is detected. The band ratios remain constant, and the intensities of the polymer bands increase. The difference is the overall intensity of the spectrum which decreased by a factor of about 2.

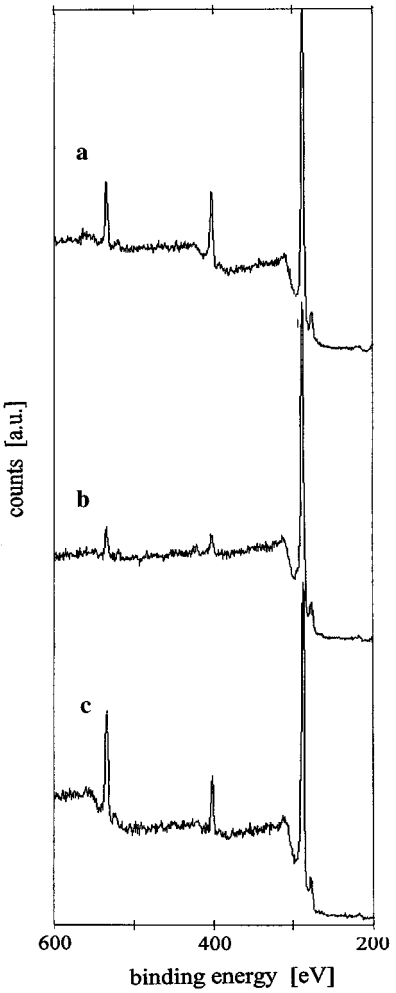

Figure 7. X-ray photoelectron core level spectra of the triazeno polymer: (a) untreated; (b) after 60 pulses with 36 mJ cm^{-2} at 248 nm; (c) after 2500 pulses with 9 mJ cm^{-2} at 248 nm. The peaks at 285 eV correspond to the C 1s, at 400 eV to the N 1s, and at 532 eV to the O 1s band.

For the irradiation with the high energy at 248 nm (e), where a surface blackening is observed, no polymer could be detected, partially due to the low signal to noise ratio in the defocused mode, which is 10 times less than for the focused mode. It was also not possible to detect bands which are specific for graphite species, even with the use of standard Raman experiments with the excitation wavelength of an Ar^+ (or Kr^+) laser.

X-ray Photon Spectroscopy (XPS). In order to get more information about the chemical changes of the polymer surface, high-vacuum surface spectroscopic techniques were used. For XPS measurements the analytical depth is on the order of 50 nm and should therefore be more sensitive to surface modifications than FT-Raman spectroscopy. The XPS spectra before and after irradiation at 248 nm is shown in Figure 7. The experimental values derived from the peak area of the different atoms were different from the stoichiometric values, a quite common feature for polymers due to surface contamination additives or differences between surface and bulk composition.[19] In this first study of the triazeno polymers it was not the aim to resolve the XPS spectra in detail. The aim was to study relative changes of the surface composition after laser treatment. For this reason the changes are shown in percent relative to untreated polymer, for which the atomic ratios are set to 100%. As a result we did not try to fit the peaks according to the different oxidation states of

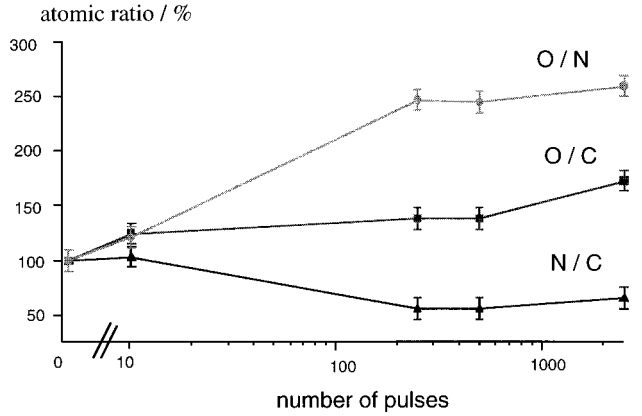

Figure 8. Atomic ratios in percent of the triazeno polymer after irradiation with various pulse numbers with 9 mJ cm^{-2} at 248 nm.

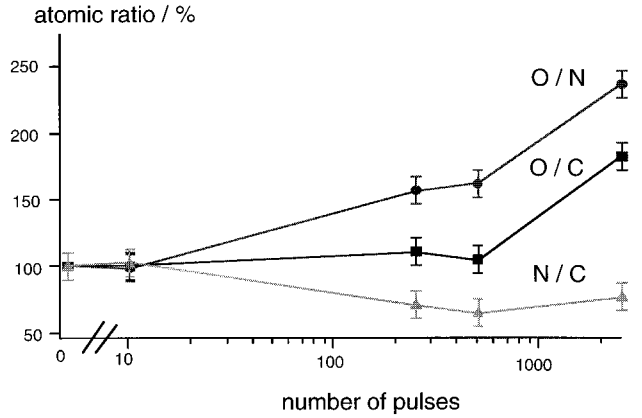

Figure 9. Atomic ratios in percent of the triazeno polymer after irradiation with various pulse numbers with 10 mJ cm^{-2} at 308 nm.

the atoms. Additionally, there is a lack of reference data for polymers with N=N bonds. It is known for nitrogen compounds that the shake up satellites can account for up to 30% of the peak intensity and are difficult to observe because they are masked by the inelastic loss structure.[20,21] Nevertheless, the N 1s peak is still a function of the single- and double-bonded nitrogen and therefore an excellent probe for changes of the nitrogen content. The relative changes of the O/N, O/C, and N/C atomic ratios after laser treatment were used to analyze the surface modifications.

The irradiation with fluences below the threshold of ablation revealed similar behaviors for both irradiation wavelengths. In the case of 248 nm irradiation (Figure 8) an increase of O/N and O/C is detected, whereas the N/C ratio decreases. The main changes of the ratio take place during the first 250 pulses and then stay constant up to 2500 pulses. The increases of the two oxygen ratios show clearly that the surface has a higher O content than before the irradiation. It is also determined that the N functionalities are preferentially removed. In the case of the 308 nm irradiation (Figure 9) the same kind of changes of the ratios are found, namely, the increase of the O/N and O/C ratios. The main difference is that constant values are not reached. After 2500 pulses all ratios reach values similar to those for 248 nm irradiation.

For irradiation with fluences above the threshold of ablation a totally different behavior is detected. For 248 nm (KrF laser) irradiation only the O/N increases, whereas the O/C and N/C ratios decrease (Figure 10).

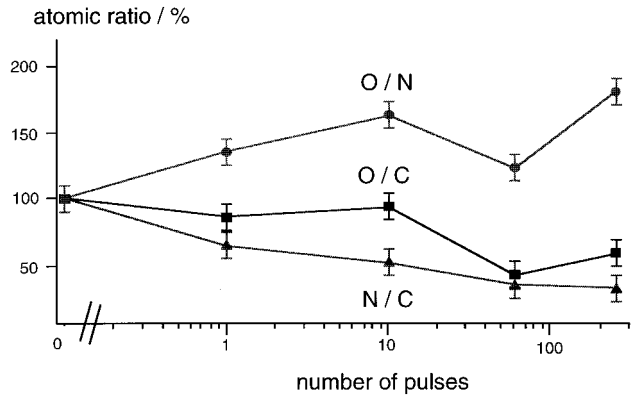

Figure 10. Atomic ratios in percent of the triazeno polymer after irradiation with various pulse numbers with 36 mJ cm^{-2} at 248 nm.

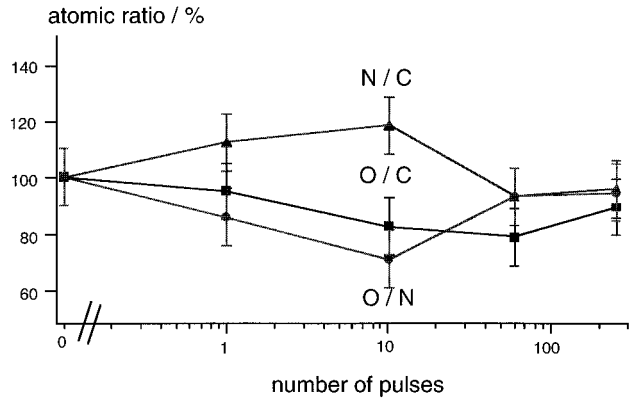

Figure 11. Atomic ratios in percent of the triazeno polymer after irradiation with various pulse numbers with 30 mJ cm^{-2} at 308 nm.

Particularly, the decrease of the O/C ratio shows that no surface oxidation takes place but rather a carbonization. Surface carbonization was also found with XPS for the irradiation of polyimide with 193 nm.[22] The two other ratios indicate again the release of nitrogen. This is in agreement with the nonpolar surface measured with the contact angle and the black appearance of the polymer films after irradiation.

In the case of 308 nm irradiation with fluences above the threshold of ablation the most complex behavior is found (Figure 11). Only minor changes took place between 1 and 10 pulses. These changes can be attributed to removal of oxygen and carbon surface contaminations. In addition the largest roughening of the surface (Figure 2a) is detected for 10 pulses, which can also influence the relative atomic ratios. After more than 10 pulses the atomic ratios approach, within the error of the experiment, the starting values. This indicates that no surface modification took place and the polymer is ablated layer by layer.

In additional to XPS we tried static SIMS to get more information about the nature of the surface modifications. SIMS has the advantages of a smaller sampling depth (1 nm as compared to the 550 nm of XPS) and direct chemical information in the spectra. The problems are the quantification of spectra and the complex data acquisition.[23,24] In the positive as well as in the negative SIMS spectra no new peaks appeared after laser irradiation. In the positive SIMS spectra, the peaks could be assigned to the typical aliphatic CH and some aromatic CH fragments.[24] After irradiation the higher molecular weight fragments (>70) could not be detected. The overall intensities of the spectra were reduced after laser irradiation. For both wavelengths the reduction was higher for irradiation with fluences above the threshold and for 248 nm higher than for 308 nm irradiation. In the case of 308 nm irradiation with fluences above the threshold of ablation the reduction was only about one-third. This indicates that either the small changes of the atomic ratios have a pronounced influence on the SIMS spectra or that changes at the surface take place without changing the atomic ratios. An example for this would be cross-linking of the polymer chains, resulting in an overall decrease of the SIMS intensities. Due to the reduced intensities it is not possible to detect higher molecular weight fragments. Nevertheless there are no new peaks, indicating a surface modification, and the reduction of the intensity is only minor and close to the instrumental error.

For the 248 nm irradiation above the threshold of ablation the intensity of the spectra were reduced drastically ($^1/_{30}$th). This can be assigned to a shielding effect of the carbon species at the surface of the polymer, as detected with the other spectroscopic techniques.

The negative SIMS spectra showed only low molecular weight fragments, like CH^-, CH_2^-, C_2H^-, and CN^- before irradiation. After irradiation the overall intensity was only reduced slightly (10−30%). These values are close to the instrumental error but might be due to a fragmentation of the polymer at the surface, which would have only a minor influence on the intensity of the low molecular weight fragments.

Discussion

A mechanism for the laser irradiation of the triazeno polymer is outlined in Scheme 1.

Fluences below the Threshold of Ablation. First we discuss the changes of the polymer after irradiation with laser fluences below the threshold of ablation. The SEM pictures have shown that no changes of the surface morphology after irradiation took place. From the UV measurements decomposition of the triazeno chromophore can be seen as demonstrated by the decrease of the absorption maximum at 330 nm. The UV spectra for 248 and 308 nm irradiation revealed a difference in the curves (shown in Figure 1). For 248 nm irradiation the absorption decreased continuously to a curve which remained nearly constant after 500 pulses (Figure 1c). In the case of 308 nm irradiation, the absorption first decreased, similar to 248 nm irradiation, but then after more than 250 pulses an overall (from 190 to 1000 nm, partly shown in Figure 1b) increase of the absorption is detected. The broad appearance of the absorption over the whole UV−vis range suggests that this is not due to the formation of new absorption bands, but to a "scattering" effect. The SEM pictures have shown that there is no surface roughening; therefore it must be caused by an "internal" roughening from gaseous bubbles, trapped in the polymer matrix and probably filled with nitrogen (Scheme 1, step 5). The nitrogen is a product of the photolytic decomposition of the triazene bond, creating an unstable radical, which decomposes on a very fast time scale[25] (shown in steps 1 and 2 in Scheme 1). Even with ESR spin trap experiments it was not possible to detect a diazo radical, resulting from the photolysis of aryl−dialkyltriazenes.[26] The increase of the absorption over the whole range from 190 to 1000 nm also suggests a size distribution of the bubbles inside the polymer matrix in the same range. In the FT-Raman spectra of the polymer after irradiation with 10 000 pulses at 308

Scheme 1. Proposed Mechanism for the Decomposition of the Triazeno Polymer after Laser Irradiation with 248 and 308 nm

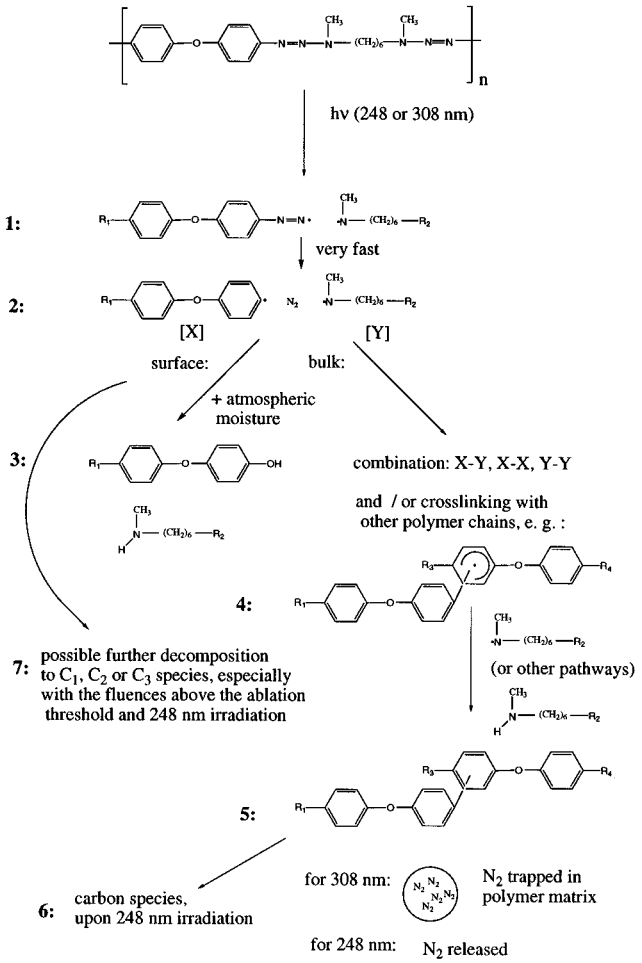

nm with 10 mJ cm^{-2} (Figure 6b) an increase of all polymer bands was detected. This behavior could also be due to an increase of the scattering of the laser light. The extended Kubelka−Munk theory for Raman scattering shows that the relative intensity of the Raman spectra is a function of the absorption coefficient and the scattering coefficient.[18] Under certain conditions an increase of the scattering can lead to an increase of the relative intensity of the Raman spectra.[27] The SEM pictures have shown that there is no roughening of the surface, and the UV spectra have indicated that "internal" scattering is present. Therefore it can be assumed that this could be the reason for the increased intensity of the polymer bands and the decrease of the "background" in the FT-Raman spectra. The irradiation is thought to create "microbubbles" of trapped nitrogen, released from the photolytic decomposition of the triazene chromophore. The bubbles reach sizes up to 1 μm, causing the scattering of the laser excitation light (1064 nm). For 248 nm irradiation no internal scattering was detected in the UV and FT-Raman spectra. The Raman spectra (Figure 6c) showed a decomposition of the triazeno chromophore, as derived from the decrease of the intensity of this band, and an increase of the baseline. A baseline increase is a typical feature for a thermal load of the sample during the FT-Raman measurement. This is caused by the absorption of the laser light (1064 nm).

To explain the difference between the 248 and 308 nm irradiation, some properties of the polymer and laser at the two irradiation wavelengths must be discussed. At 248 nm the penetration depth of the laser is about 150 nm, whereas for 308 nm the penetration depth is only 60 nm. In addition the photon energy at 248 nm is 5 eV as compared to the 4 eV at 308 nm. This is one of the reasons why the quantum yield (QY) of photolysis in solution for 248 nm is higher (1.5%) than for 308 nm (0.22%).[7] A closer inspection of the UV spectra (Figure 1) reveals that 248 nm is at a minimum of the absorption curve. Assuming a Lorentzian profile for the different absorption bands it is obvious that an irradiation with 248 nm can lead to a direct excitation of the absorption bands below and above 248 nm.

The higher QY results in a faster decomposition of the polymer and therefore a higher partial pressure of the nitrogen inside the polymer matrix. The pressure is released and no gaseous bubbles are developed. In addition 248 nm irradiation is capable of exciting the aromatic system and has sufficient energy to decompose C−C bonds.

Therefore we suggest the following steps for the bulk decomposition of the polymer after irradiation with fluences below the threshold of ablation. First the photolabile triazeno group is decomposed, with nitrogen as the first product (Scheme 1, steps 1 and 2). This is confirmed with the decreasing N content in the XPS spectra (Figure 8 and 9). Then the phenyl and amino radicals created inside the polymer matrix can combine or lead to a cross-linking or branching of the polymer, as shown for cross-linking in steps 4 and 5 of Scheme 1. It was suggested that cross-linking will lead to a peak broadening in the XPS spectra.[28] We also detected some broadening of the peaks after irradiation and found some insoluble residues for thick films, indicating a polymer network. The decreased intensity of the SIMS spectra also indicated a polymer network. In addition it was demonstrated that the structurally related monomeric bis(triazeno) compounds can be used as thermal cross-linkers for polyimides and aromatic polymers.[29] Therefore only cross-linking is shown in Scheme 1.

The cross-linked polymer still has an absorption at 248 nm. Excessive irradiation with 248 nm can therefore result in some further decomposition of the cross-linked polymer or other possible products, like branched systems or amines (Scheme 1, step 4). The main products of such a process are carbon species, which will absorb at 1064 nm, as revealed by the thermal load in the FT-Raman spectra.

At the polymer surface the radical species (Scheme 1, step 1 and 2) can react with atmospheric moisture to form surface hydroxyl groups (shown in step 3). The existence of polar groups, like −OH, at the surface is clearly shown in the contact angle measurements where a decrease of the water contact angle is detected (Figure 4). In the XPS measurements an increase of the oxygen content is revealed (Figures 8 and 9), which confirms a surface oxidation of the polymer.

Fluences above the Threshold of Ablation. The main difference between the irradiation of the triazeno polymer with low and high fluences is a clear change in the polymer response. There is no simple photochemical mechanism acting alone but in addition material is removed (ablation) corresponding to a much higher QY as for the normal photolysis.[30] The UV spectra of the films could not give any valuable information because the films were totally removed during ablation. Therefore thicker films were used, revealing a pronounced difference between the two irradiation

wavelengths. Optical inspection of the films after multiple pulses at 248 nm showed a black appearance, whereas no darkening took place after 308 nm irradiation. The SEM pictures revealed also a different appearance of the polymer surface after irradiation with the two lasers. For 308 nm irradiation, microstructures with an increasing intensity were found, but after more than 10 pulses the trend was reversed and the microstructures became less pronounced (Figure 2). After 248 nm irradiation the microstructures were also observed. There was no decrease of their intensity and some "treelike" structures were found on the top of the microstructures (Figure 3). Microstructures of polymers were reported previously for subthreshold irradiation of polymers with polarized laser beams for controlled roughening of the surface with various laser irradiation wavelengths.[31] With fluences above the threshold of ablation it is also possible to create microstructures.[32] These features are found for films and fibers and are attributed to different mechanisms like Marangoni convection,[33] surface scattered waves,[34] recombination of microcracks[35] and a mixture of several mechanisms.[36] It is also known that the irradiation of stretched polymers results in the creation of microstructures due to the release of the stress fields[37] upon laser irradiation and surface melting, which leads to an amorphization of crystalline polymers.[38]

Pronounced differences between the microstructures created with different irradiation wavelengths above the threshold of ablation with similar fluences have not been reported to our knowledge. Assuming that the decomposition mechanism of the triazeno polymer does not change totally in the case of ablation, but results in mainly material removal at a higher rate and some possible variations to the mechanism, we suggest a different mechanism for the microstructures. As for the low irradiation fluence, the XPS spectra and the nonsoluble residues after irradiation suggest a cross-linking mechanism (step 5 in the scheme). In addition, parts of the polymer and low molecular weight fragments are removed during ablation. Thus a polymer network, with lower volume, remains with the appearance of the "nap" structures. The treelike structures on the top of the nap are the result of a further polymer decomposition. There are two possibilities for this: a decomposition of the cross-linked polymer or a complete decomposition of the ablated fragments, which are redeposited. It was shown that in the case of polyimide ablation carbon clusters remained. These clusters can have a molecular weight of up to 5000 and sometimes include heteroatoms, such as nitrogen.[39−42] With time-of-flight measurements, fullerenes have been found in the ablation plume.[38−42] The fullerenes can only be formed from a complete fragmentation to C_1, C_2, and C_3 fragments,[43] which have been found with laser-induced fluorescence measurements.[44] Whether the tree like structures are formed by the redeposition of plume particles or by remaining carbon clusters is not clear. Graphite and amorphous carbon were identified on polyimide (PI) after laser irradiation (308 nm) with Raman spectroscopy of single black particles.[45] The carbonized PI surface showed increased conductivity[46] and is suggested to be the result of a thermal mechanism leading to fused ring structures (248 nm irradiation).[47] For laser irradiation (248 nm) of chlorinated poly(vinyl chloride) no graphitization was found but polyene and polyyne structures were detected with Raman spectroscopy.[48]

We tried to assign the carbon species to one of the above mentioned forms, but due to the low intensities of these bands and the "treelike" structure (SEM picture), which cover the surface only partly, we were not able to assign the carbon in detail. Nevertheless we believe that a carbonization of the surface took place. The contact angle measurements have shown a drastic increase of the contact angle (Figure 5), as expected for a very unpolar surface like, *e.g.*, graphite. The XPS spectra have also confirmed carbonization of the surface for 248 nm irradiation (Figure 10).

For 308 nm irradiation a different behavior is found. The XPS spectra and contact angle measurements showed nearly no changes of the surface after irradiation. The small variation can be explained by the initial development of the microstructures, which became less pronounced after several pulses. The XPS spectra showed that the surface has nearly the same chemical composition as the starting material. This suggests that the polymer is removed completely layer by layer without altering the remaining material. The FT-Raman spectra have shown only an overall decrease of all polymer bands, indicating a decrease of the polymer thickness. A possible explanation is again the different penetration depth of the laser. In the case of 308 nm irradiation the whole laser energy is concentrated in a thin layer and mainly the photolabile triazeno group is excited and decomposed. The initial microstructures could be the result of some cross-linking in the early stages of ablation. A possible reason for this is shielding effects of surface contaminations which must be removed first. After several pulses these contaminations are removed and the polymer is ablated completely. The lack of debris[7,13] after ablation and the absence of any solid or liquid fragments in the ablation plume,[49] as revealed by nanosecond photography, suggest further fragmentation of the ablation products (Scheme 1, step 7). In conclusion we suggest that for 308 nm irradiation the polymer is ablated layer by layer with no modification of the polymer bulk.

Conclusion

It was demonstrated with surface analysis techniques that the polymer surface is modified selectively with different laser irradiation wavelengths. The two laser energy regimes, above and below the threshold for laser ablation, reveal pronounced differences. For both irradiation wavelengths (248 and 308 nm) the polymer surface modification is solely chemical after treatment with fluences below the threshold. Each irradiation wavelength leads to a surface oxidation, as shown with the contact angle and XPS measurements. The oxidation is a result of the radical pathway of photodecomposition of the triazeno chromophore.

At fluences above the threshold of ablation for each wavelength a different behavior is observed. After irradiation at 248 nm, growing "naplike" structures are detected, possibly a result of cross-linking of the polymer. The surface appeared black and carbonized, suggesting a variation of the mechanism of the low fluence irradiation. The polymer is only partly removed, due to the higher penetration depths. The remaining cross-linked polymer can be decomposed to carbon species, especially with the higher photon energy of the 248 nm laser.

In the case of 308 nm irradiation, first some microstructures are created, but the ablated surface becomes smooth again after some pulses. The chemical composi-

tion also remained unchanged after several pulses, suggesting a photochemical mechanism, removing the polymer completely layer by layer without any redeposition of ablation products.

References and Notes

(1) *Lasers in Polymer Science and Technology: Applications;* Fouassier, J.-P., Rabek, J. F., Eds.; CRC Press: Boca Raton, FL, 1990; Vol. I−IV.
(2) Jain, K. *Excimer Laser Lithography;* SPIE-The International Society for Optical Engineering; Bellingham, WA, 1990.
(3) (a) Kawamura, Y.; Toyoda, K.; Namba, S. *Appl. Phys. Lett.* **1982**, *40*, 374. (b) Srinivasan, R.; Mayne-Banton, V. *Appl. Phys. Lett.* **1982**, *41*, 578.
(4) Lazare, S.; Granier, V. *Laser Chem.* **1989**, *10*, 25.
(5) Srinivasan, R.; Braren, B. *Chem. Rev.* **1989**, *89*, 1303.
(6) Masuhara, H.; Fukumura, H. *Polym. News* **1991**, *17*, 5.
(7) Lippert, T.; Stebani, J.; Ihlemann, J.; Nuyken, O.; Wokaun, A. *Angew. Makromol. Chem.* **1993**, *206*, 97.
(8) Lippert, T.; Stebani, J.; Ihlemann, J.; Nuyken, O.; Wokaun, A. *Angew. Makromol. Chem.* **1993**, *213*, 127.
(9) E.g.: Brannon, J. H. J. *J. Vac. Sci. Technol.* **1989**, *B7*, 1064. von Gutfeld, R. J. Srinivasan, R. *Appl. Phys. Lett.* **1987**, *51*, 15. Seeger, D. E.; Rosenfield, M. G. *J. Vac. Sci Technol.* **1988**, *B6*, 399. Singleton, D. L.; Paraskevopoulos, G.; Irwin, R. S. *J. Appl. Phys.* **1989**, *66*, 324. Koren, G.; Donelon, J. J. *J. Appl. Phys.* **1988**, *B45*, 45.
(10) Stebani, J.; Nuyken, O.; Lippert, T.; Wokaun, A. *Makromol Chem., Rapid Commun.* **1993**, *206*, 97.
(11) Stebani, J.; Nuyken, O.; Lippert, T.; Wokaun, A.; Stasko, A. *Makromol Chem. Phys.* **1995**, *196*, 751.
(12) Stebani, J.; Nuyken, O.; Lippert, T.; Wokaun, A.; Stasko, A. *Makromol Chem. Phys.* **1995**, *196*, 739.
(13) Lippert, T.; Stebani, J.; Ihlemann, J.; Nuyken, O.; Wokaun, A. *J. Phys. Chem.* **1993**, *97*, 12296.
(14) Lippert, T.; Bennett, L. S.; Nakamura, T.; Niino, H.; Ouchi, A.; Yabe, A. *Appl. Surf. Sci.*, in press.
(15) The term "blackening of the surface" was used because during the contact angle measurements the water droplets turned black. This shows that at least a large part of the "black" appearance is located at the surface.
(16) Lazare, S.; Granier, S.; Lutgen, F.; Feyder, G. *Rev. Phys. Appl.* **1988**, *23*, 1065.
(17) Zimmermann, F.; Lippert, T.; Beyer, C.; Stebani, J.; Nuyken, O.; Wokaun, A. *Appl. Spectosc.* **1993**, *47*, 931.
(18) Schrader, B.; Moore, D. S. *IUPAC Recommendations Anal. Chem. Div.* **1995**, 12.
(19) Beamson, G.; Briggs, D. *High Resolution XPS of Organic Polymers*; John Wiley & Sons: Chichester, U.K., 1992. Clark, D. T. *Pure Appl. Chem.* **1985**, *57*, 941.
(20) Gelius, U. *J. Electron. Spectrosc. Relat. Phenom.* **1974**, *5*, 985.
(21) Beamson, G.; Briggs, D. *Mol. Phys.* **1992**, *76*, 919.
(22) Brezini, A.; Zekri, N. *J. Appl. Phys.* **1994**, *75*, 2015.
(23) Briggs, D. *Br. Polym. J.* **1989**, *21*, 3.
(24) Briggs, D.; Brown, A.; Vickermann, J. C. *Hanbook of Static Secondary Ion Mass Spectrometry*; John Wiley & Sons: Chichester, U.K., 1989.
(25) Lippert, T.; Stebani, J.; Stasko, A.; Nuyken, O.; Wokaun, A. *J. Photochem. Photobiol.* **1994**, *78*, 139.
(26) Stasko, A.; Adamcik, V.; Lippert, T.; Wokaun, A.; Dauth, J.; Nuyken, O. *Makromol. Chem.* **1993**, *194*, 3385.
(27) Schrader, B.; Bergmann, G. *Fresenius Z. Anal. Chem.* **1967**, *225*, 230.
(28) Novis, Y.; De Meulemeester, R.; Chtaïb, M.; Pireaux, J.-J.; Caudano, R. *Brit. Polym. J.* **1989**, *21*, 147.
(29) Lau, A. N. K.; Vo, L. P. *Macromolecules* **1992**, *25*, 7294.
(30) Lippert, T.; Bennett, L. S.; Nakamura, T.; Niino, H.; Ouchi, A.; Yabe, A. *Appl. Phys. A*, in press.
(31) Bolle, M.; Lazare, S.; Leblanc, M.; Wilmes, A. *Appl. Phys. Lett.* **1992**, *60*, 674. Bolle, M.; Lazare, S. *Appl. Surf. Sci.* **1993**, *69*, 31.
(32) Dyer, P. E.; Farley, R. J. *Appl. Phys. Lett.* **1990**, *57*, 765.
(33) Bahners, T.; Schollmeyer, E. *J. Appl. Phys.* **1989**, *66*, 1884.
(34) Dyer, P. E.; Farley, R. J. *J. Appl. Phys.* **1993**, *74*, 1442.
(35) Tonyali, K.; Jensen, L. C.; Dickinson, J. T. *J. Vac. Sci. Technol.* **1988**, *A6*, 941.
(36) Arenholz, A.; Wahner, M.; Heitz, J.; Bäuerle, D. *Appl. Phys.* **1992**, *A55*, 119.
(37) Lippert, T.; Zimmermann, F.; Wokaun, A. *Appl. Spectosc.* **1993**, *47*, 1931.
(38) Dunn, D. S.; Ouderkirk, A. J. *Macromolecules* **1990**, *23*, 770.
(39) Creasy, W. R.; Brenna, J. T. *J. Chem. Phys.* **1990**, *92*, 2269.
(40) Otis, C. E. *Appl. Phys. B* **1989**, *49*, 455.
(41) Campbell, E. E. B.; Ulmer, G.; Hasselberger, B.; Busmann, H.-G.; Hertel, I. V. *Appl. Surf. Sci.* **1989**, *43*, 346.
(42) Campbell, E. E. B.; Ulmer, G.; Hasselberger, B.; Hertel, I. V. *J. Chem. Phys.* **1990**, *93*, 6900.
(43) Singleton, D. L.; Paraskevopoulos, G.; Irwin, R. S. *J. Appl. Phys.* **1989**, *66*, 3324.
(44) Srinivasan, R.; Braren, B.; Seeger, D. E.; Dreyfus, R. W. *Macromolecules* **1986**, *19*, 916.
(45) Gu, X. J. *Appl. Phys. Lett.* **1993**, *62*, 1568.
(46) Schumann, M.; Sauebrey, R.; Smayling, M. C. *Appl. Phys. Lett.* **1991**, *58*, 428.
(47) Feurer, T.; Sauerbrey, R.; Smayling, M. C.; Story, B. J. *Appl. Phys.* **1993**, *A56*, 275.
(48) Shimoyama, M.; Niino, H.; Yabe, A. *Makromol. Chem.* **1992**, *193*, 569.
(49) Bennett, L. S.; Lippert, T.; Furutani, H.; Fukumura, H.; Masuhara, H. *Appl. Phys. A*, in press.

MA9517198